Research Paper

Depletion of ceramides with very long chain fatty acids causes defective skin permeability barrier function, and neonatal lethality in ELOVL4 deficient mice

Wenmei Li[1], Roger Sandhoff[2], Mari Kono[1], Patricia Zerfas[3], Vickie Hoffmann[3], Bryan Char-Hoa Ding[1], Richard L. Proia[1] and Chu-Xia Deng[1]

1. Genetics of Development and Disease Branch, National Institute of Diabetes and Digestive and Kidney Disease, National Institutes of Health, 10 Center Drive, Bethesda, MD 20892, USA.
2. Cellular and Molecular Pathology (E090), German Cancer Research Center, Heidelberg, Germany.
3. Division of Veterinary Resources, Office of Research Services, National Institutes of Health, Bethesda, MD 20892, USA.

Correspondence to: Chu-Xia Deng, Phone: 301-402-7225, Fax: 301-480-1135, Email: chuxiad@bdg10.niddk.nih.gov

Very long chain fatty acids (VLCFA), either free or as components of glycerolipids and sphingolipids, are present in many organs. Elongation of very long chain fatty acids-4 (ELOVL4) belongs to a family of 6 members of putative fatty acid elongases that are involved in the formation of VLCFA. Mutations in ELOVL4 were found to be responsible for an autosomal dominant form of Stargardt's-like macular dystrophy (STGD3) in human. We have previously disrupted the mouse *Elovl4* gene, and found that *Elovl4+/-* mice were developmentally normal, suggesting that haploinsufficiency of ELOVL4 is not a cause for the juvenile retinal degeneration in STGD3 patients. However, *Elovl4-/-* mice died within several hours of birth for unknown reason(s). To study functions of ELOVL4 further, we have explored the causes for the postnatal lethality in *Elovl4-/-* mice. Our data indicated that the mutant mice exhibited reduced thickness of the dermis, delayed differentiation of keratinocytes, and abnormal structure of the stratum corneum. We showed that all *Elovl4-/-* mice exhibited defective skin water permeability barrier function, leading to the early postnatal death. We further showed that the absence of ELOVL4 results in depletion in the epidermis of ceramides with ω-hydroxy very long chain fatty acids (≥C28) and accumulation of ceramides with non ω-hydroxy fatty acids of C26, implicating C26 fatty acids as possible substrates of ELOVL4. These data demonstrate that ELOVL4 is required for VLCFA synthesis that is essential for water permeability barrier function of skin.

Key words: ELOVL4, lipid, epidermis, keratinocyte differentiation, stratum corneum

1. Introduction

Mammalian skin consists of a dermis and an epidermis. Keratinocytes in the basal layer of the epidermis are epidermal precursor cells that undergo both continuous proliferation to maintain their population and differentiation when they migrate in the direction of the skin surface [1,2]. The sequential differentiation of keratinocytes results in the formation of several anatomically distinct layers, including the stratum basale, the stratum spinosum, the stratum granulosum and the stratum corneum [3]. The stratum corneum (SC) is the outermost layer of the epidermis and serves as a barrier for transepidermal water loss that is essential to prevent dehydration. Ceramides, a class of sphingolipids with a sphingoid base in amide linkage with a fatty acid, are major and essential components of the water barrier in epidermis [3-6]. A substantial portion of epidermal ceramides contain ω-hydroxy long chain fatty acids (C≥28), which can be in the form of linoleic acid acyl esters or bound to protein [7,8].

Elongation of very long chain fatty acids-4

(ELOVL4) belongs to a family that consists at least 6 putative fatty acid elongases in mouse and human [9]. The *ELOVL4* gene encodes a putative 314 aa protein that is highly conserved through evolution [10,11]. ELOVL4 is expressed in brain, retina, skin, lens, and testis in mice [12]. Mutational analysis of the *ELOVL4* gene in patients suffering Stargardt's macular dystrophy 3 (STGD3) detected a 5 bp deletion, which results in a frame-shift that truncates 51 aa from the C-terminal end of ELOVL4 [13-15]. STGD3 is an autosomal dominant juvenile retinal disease characterized by progressive accumulation of lipofuscin, atrophy of the retinal pigment epithelium, and degeneration of macular photoreceptors [13,16,17]. Consistent with a view that the 5-bp deletion of the *ELOVL4* gene is responsible for the STGD3, mice either over expressing a 5-bp *ELOVL4* deletion transgene in retina driven by a human photoreceptor-specific promoter of the gene encoding interphotoreceptor retinoid-binding protein (*IRBP-ELOVL4*) ([18], Li and Deng unpublished data), or carrying a targeted 5-bp *ELOVL4* deletion in heterozygous state (*Elovl4+/del*) [19]

recapitulate major features of the retinal pathogenesis in STGD3 patients.

To study function of ELOVL4, we have generated a candidate null mutation by inserting of a neo cassette [20] into the exon 2 of the *Elovl4* locus [21]. Our analysis indicated that mice heterozygous for the mutation (*Elovl4*$^{+/-}$) were developmentally normal and did not exhibit apparent photoreceptor degeneration up to 11 months of age [21]. Because the *Elovl4*$^{+/del}$ mice and *IRBP-ELOVL4* transgenic mice develop early onset of photoreceptor ultrastructural abnormalities, while the *Elovl4*$^{+/-}$ mice are normal, this observation suggests that a dominant negative effect, rather than haploinsufficiency, is the primary mechanism of juvenile retinal degeneration in STGF3 patients.

Notably, we also found that *Elovl4*$^{-/-}$ mice, while exhibiting normal retinal development, died several hours after birth due to unknown causes [21]. These data suggest that ELOVL4 is indispensable for the early stages of postnatal survival. Here we have further analyzed *Elovl4*$^{-/-}$ mice and found that they all displayed profound skin atrophy and impaired water insulation function. The mutant mice also lacked ceramides with ω-hydroxy very long chain fatty acids ($\geq$C28) indicating that ELOVL4 is critical for the formation of epidermal-specific sphingolipids with essential permeability barrier function.

2. Materials and Methods

Mice

Mice carrying a heterozygous mutation of Elovl4 (*Elovl4*$^{+/-}$) were genotyped as described [21]. The *Elovl4*$^{+/-}$ mice were interbred to generate *Elovl4*$^{-/-}$ mice, which were collected at birth and were subjected to various analyses described in the text. All the mice were in a mix background of 129SVEV and Black Swiss at a roughly 1:1 ratio. Animal care is in accordance with guidelines of animal user and care committee of NIDDK.

Histology and immunohistochemical staining

For histology, tissues were fixed in 10% formalin, blocked in paraffin, sectioned, stained with hematoxylin and eosin, and examined by light microscopy. Detection of primary antibodies was performed using the ZYMED Histomouse™ SP Kit according to the manufacturer's instructions. Antibodies for involucrin, loricrin, filaggrin, K14, and K6 were purchased from Covance Inc.

Skin permeability assay

The unfixed the newborn pups were incubated for 5 min in methanol, rinsed with PBS, and followed by incubation in 0.5% hematoxylin for 30 min.

Electronmicroscopy

Pancreas tissue was fixed in 2% glutaraldehyde in 0.1 M cacodylate buffer, pH 7.4, overnight at 4°C. The tissue was washed with cacodylate buffer and postfixed with 1% OsO$_4$ tetroxide for two hours. Tissue was washed again with 0.1 M cacodylate buffer,

serially dehydrated in ethanol and propylene oxide and embedded in Eponate 12 resin (Ted Pella, Redding, CA, USA). Thin sections, approx. 80 nm, were obtained by utilizing the Leica ultarcut-UCT ultramicrotome (Leica, Deerfield, Ill., USA) and placed onto 300 mesh copper grids and stained with saturated uranyl acetate in 50% methanol and then with lead citrate. The grids were viewed in the Philips 410 electron microscope (FEI, Hillsboro, OR, USA) at 80 kV and images were recorded on Kodak S0-163 film.

Analysis of ceramids in epidermis by nanoESI-MS/MS

Sphingolipid extraction and mass spectrometric analysis were performed according to Jennemann et al. [22]. In brief, skins were trypsinized over night at 4 °C to separate epidermis from dermis. Lyophilized tissue was extracted once with chloroform/methanol/water in a ratio of 30:60:8 by vol. and twice in a ratio of 10:10:1 by vol., each for 15 at 50 °C in an ultra-sound bath. Combined extracts were desalted using reversed phase RP-18 columns. In order to cleave esterified sphingolipids, aliquots of these free extractable lipids were further saponified with 0.1 M KOH in methanol for 2 hours at 50 °C, neutralized and desalted using reversed phase RP-18 columns. In order to remove residual free lipids, the remaining protein pellets were treated 3 times with methanol at RT for 10 min and 2 times with 95 % methanol at 60 °C. From these "washed" protein pellets, protein bound lipids were released with 1 M KOH in 95 % methanol at 60 °C for 2 hours. Supernatant was neutralized with 1 M acetic acid, dried and desalted using reversed phase RP-18 columns. Quantification of sphingolipids was performed by nanoESI-MS/MS using a precursor ion scan of m/z +264 for ceramide- and GlcCer-detection (collision energy: 50 eV) as described by Sandhoff et al. 2002 [23] with slight modifications: Starting with 35 V at m/z = 500, the cone voltage was increased in a linear way up to 65 V at m/z = 1300 during the measurement. For quantification of ceramides (Cers) and GlcCers the following internal standards were added in an equimolar ratio to the samples Cer(d18:1,14:0), Cer(d18:1,19:0), Cer(d18:1,25:0), Cer(d18:1,31:0), and Cer(t18:0,31:0), and GlcCer(d18:1,14:0),GlcCer(d18:1,19:0), GlcCer(d18:1,25:0), and Cer(d18:1,31:0).

3. Results

ELOVL4 deficient mice showed defective epidermis permeability barrier function

To investigate the causes that are responsible for early postnatal lethality of the *Elovl4*$^{-/-}$ mice, we carefully monitored the newborn *Elovl4*$^{-/-}$ mice and found that all mutant mice were alive at the birth and presented a Mendelian ratio (*Elovl4*$^{-/-}$: 31, *Elovl4*$^{+/+}$: 58, *Elovl4*$^{-/-}$: 32). These mice were initially slightly smaller than wild type controls (Fig. 1A), and became more obviously smaller prior to their death within 5 hours after birth. Meanwhile, the skin *Elovl4*$^{-/-}$ mice appeared dark/purple in color and less smooth than

the skin of control (*Elovl4* wild type and heterozygous) mice (Fig. 1A). These phenotypes became progressively more severe and all mutant mice exhibited remarkable wrinkled skin a few hours after birth (Fig. 1B). The skin serves as a permeability barrier for body water loss. Therefore, we checked speed of water loss during a given period of time by measuring body weight every 30 min up to 3 and half hours. The *Elovl4*$^{-/-}$ mice lost body water at a rapid rate (~12% in 210 min), in contrast to all control mice, which maintained consistent body weight during the same period of time, suggesting the wild type skin could prevent water evaporation, but the mutant skin could not (Fig. 1C).

Next, we performed a skin permeability assay by soaking newborn mice into 0.5% hematoxilin for 30 minutes. We found that the *Elovl4*$^{-/-}$ mice were quickly stained by hematoxilin (Fig. 1D), while the dye could not penetrate the skin of control mice (Fig. 1E). These data indicate that ELOVL4 deficiency impaired the permeability barrier function of the skin, leading to the early postnatal lethal of the *Elovl4*$^{-/-}$ mice. Consistent with this, we have supplied body lotion, which reduces water loss from the skin, to 3 mutant mice and found that they all survived beyond 24 hours, although died before 36 hours after birth.

Figure 1. Defective skin water barrier function in the *Elovl4*$^{-/-}$ mice. (A, B) Appearance of *Elovl4*$^{-/-}$ (left) and control mice ~2 hours (A) and ~4 hours (B) after birth. (C) The speed of water loss. Newborn mice were weighted at the different time points as indicated. (D, E) Skin permeability assay. The *Elovl4*$^{-/-}$ mice (D) were strongly stained by 0.5% hematoxylin 5 minutes after staining, but heterozygous mice and wild type mice (E) were resistant to the staining.

ELOVL4 deficient mice showed impaired epidermis keratinocyte differentiation

Next, we performed histological analysis of the skin of newborn mice. In wild type mice, the SC is a multi-layer, loosely packed structure that is in the outermost of the skin (Fig. 2A-C). However, in the mutant mice the SC appeared thinner than control SC, and presented as split layers with varying severity in all mutant pups examined (n>10) (Fig. 2D-F, G-I), instead as a cohesive multi-layer structure in control mice (Fig. 2C). The thickness of stratum basal (Bl), spinosum (Sp), and granulosum (Gr) layers were increased (Fig. 2C, F). In addition, thickness of the dermis of the *Elovl4*$^{-/-}$ mice was reduced than that of the control mice (Fig. 2B, E, H).

To further characterize the abnormalities of mutant skin, we performed immunohistochemical staining using various lineage markers for the epidermis. The K14 marked the basal layer of keratinocytes, which are arranged as a one- or two-cell layer in the control mice (Fig. 3A), whereas in the *Elovl4*$^{-/-}$ mice, K14 expression domain was expanded to multi-cell layer (Fig. 3B). Keratinocytes located in the basal layer are precursor stem cells for the epidermis. These cells maintain their population through proliferation, and also undergo continuous differentiation to generate cells for other layers above. The expansion of basal layer keratinocytes in mutant epidermis could be caused by increased cell proliferation, and/or reduced differentiation. Using BrdU incorporation assay, we did not detect an obvious increase of BrdU positive cells in the basal layer of the mutant epidermis relative to control epidermis (Fig. 3C, D). In the control basal layer, BrdU positive cells maintained, in most case, within the
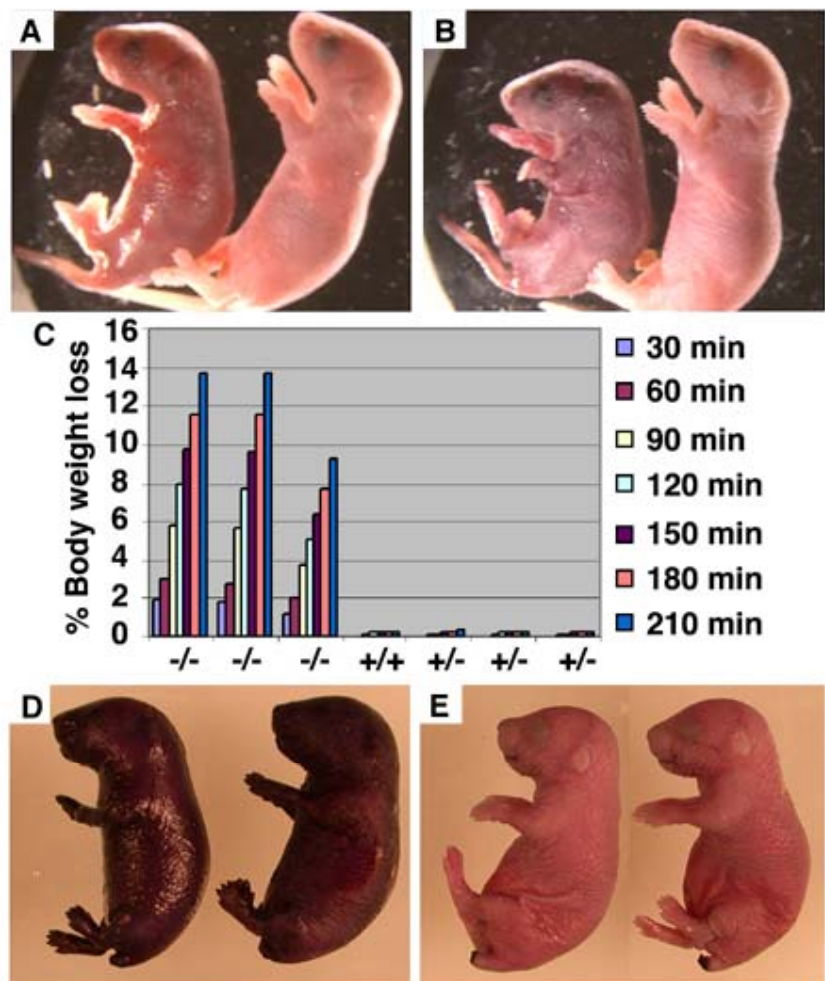
single cell layer (arrows, Fig. 3C). In contrast, the BrdU labeled mutant cells appeared in different layers (Fig. 3D), which is corresponding to the expanded K14 expression domain (Fig. 3B). In addition, the basal layer in the mutant epidermis was positively stained

by an antibody against K6, a marker for abnormal differentiation (Fig. 3F), while control epidermis was negative (Fig. 3E). These data indicate that the absence of ELOVL4 caused abnormal keratinocyte differentiation.

The SC is formed by the terminal differentiation of keratinocytes. During this process, cells sequentially incorporate precursor proteins, involucrin and loricrin, while filaggrin promotes aggregation and packing of keratin filaments to form a dense cell matrix. Our data indicated that the expression of these proteins was on primarily in the SC and upper granular in control mice (Fig. 3G, I, K). However, in the ELOVL4 knockout mice, these proteins remained in the spinous layer, and the granular layer, in addition to the SC layer (Fig. 3H, J, L). These data indicated that ELOVL4 deficiency interfered with the terminal differentiation of keratinocytes, leading to the impaired formation of the SC.

Figure 2. Abnormal skin formation of the *Elovl4*$^{-/-}$ mice revealed by H&E staining. Histology of the skin from a wild type (A-C) and two *Elovl4*$^{-/-}$ (D-I) newborn mice. Arrows in (A, D, G) point to the SC. Bars in (B, E, H) indicate the thickness of dermis. Arrows in (C, F, I) point to basal layer of the epidermis. Hf: hair follicle, Sc: stratum corneum, Gr: stratum granulosum, Sp: stratum spinosum, Bl: stratum basale. Original magnification of (A, D, G) is 100X, (B, E, H) is 200X, and (C, F, I) is 400X.
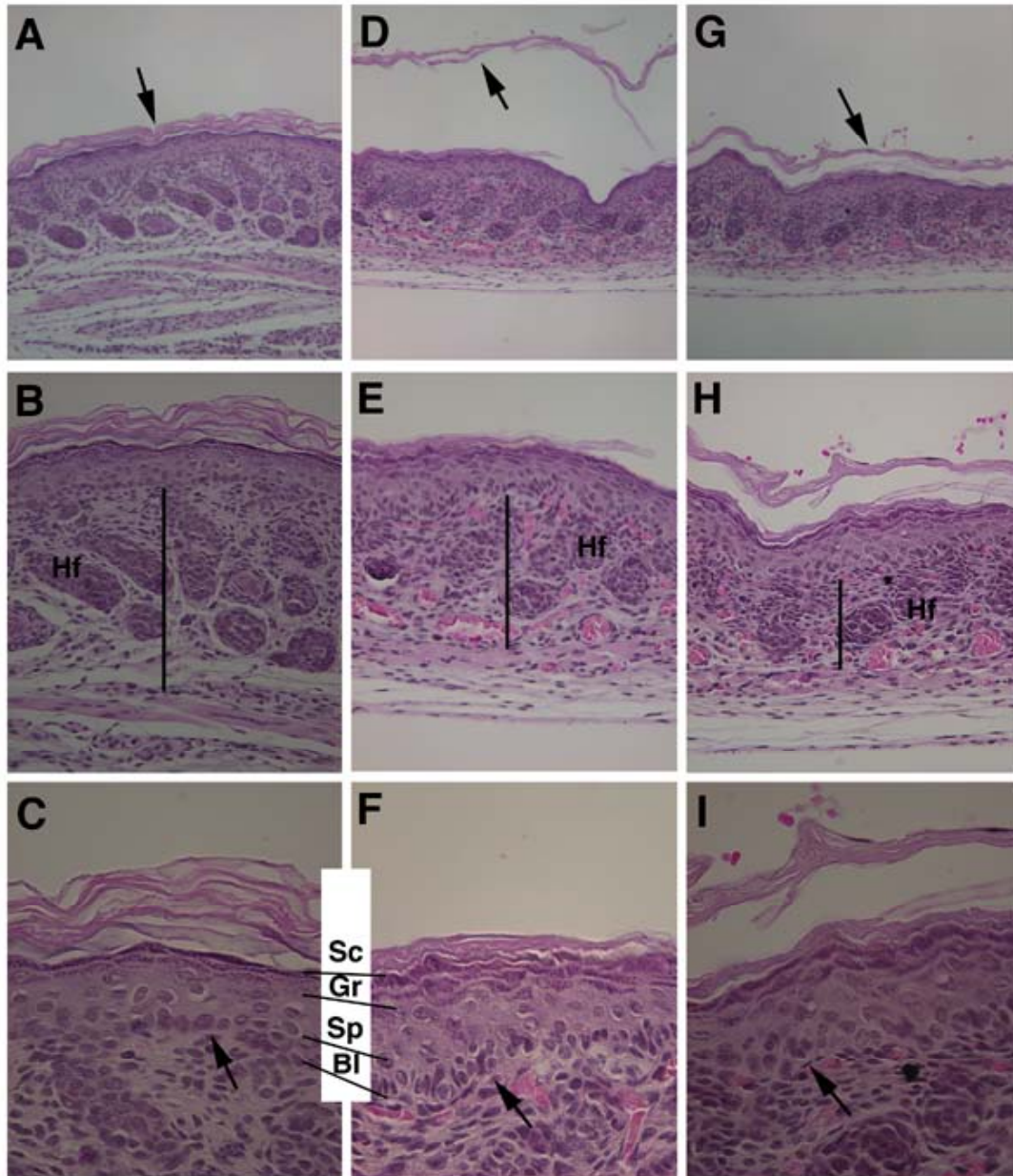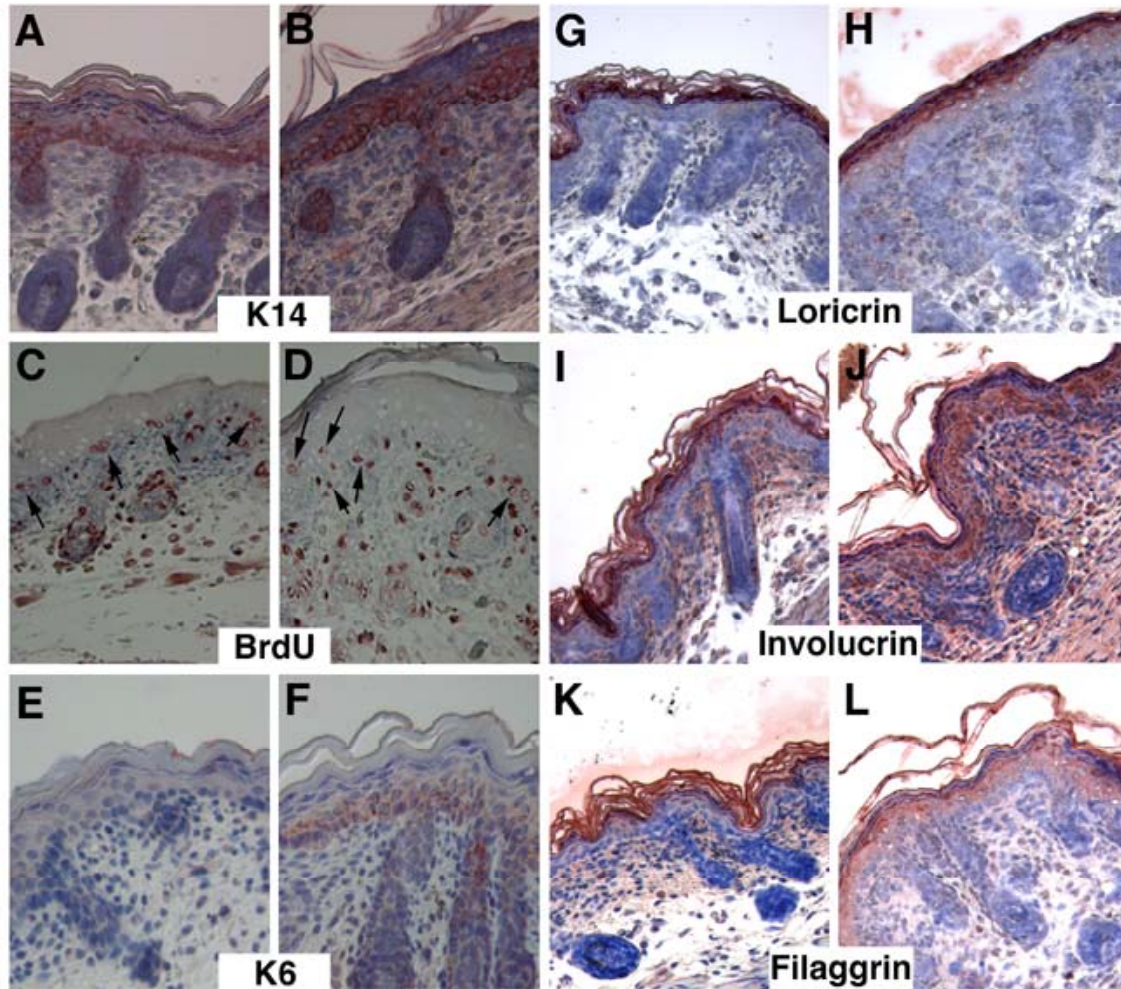
Figure 3. Delayed differentiation of keratinocytes in the skin of the *Elovl4⁻/⁻* mice. Samples shown in (A, C, E, G, I, K) are control and in (B, D, F, H, J, L) are mutant. Antibodies used were as indicated. Arrows in (C, D) point to BrdU positive cells in the basal layer of control (C) and mutant (D) epidermis.

We have noticed that, unlike the control pups, the mutant animals showed very little movement and had no desire to find the nipple and to suck milk from their mothers. Initially, we had considered whether starvation could also serve as a cause for the lethality. However, after feeding 4 mutant pups with milk purchased from supermarket through gavaging, we found it did not extend the time of survival of the mutant mice. We have also checked many other organs of mutant mice, including the brain, esophagus, heart, liver, lung, intestine, pancreas, spleen, and stomach, and did not find a consistent defect that could be responsible for the early postnatal lethality (not shown).

ELOVL4 deficiency resulted in abnormal ultrastructure in the SC

Next, we investigated if there were any ultrastructural abnormalities in the mutant epidermis using electron microscopy. The wild type SC appeared as a loosely packed basket weaved structure (Fig. 4A). In contrast, the SC of the *Elovl4⁻/⁻* mice was much more compact than control SC (Fig 4B). Our histological analysis performed earlier revealed that the SC in the *Elovl4⁻/⁻* mice was often presented as split sub-layers from the skin (Fig. 2D, G). Altogether, these data suggest that although the mutant SC is more compact, sub-layers within the SC fail to adhere, and, in most cases, peel off from the skin. No difference in the lamellar membrane at the stratum spinosum and the stratum granulosum interface was found between mutant mice and wild type (Fig. 4C, D). The basement membrane in *Elovl4⁻/⁻* mice had fewer hemidesmosomes, the attachment sites of epithelial cells to basal lamina, with shortened or missing tonofilaments (arrowheads, Fig. 4E, F). Collagenous fibrils were also sparse and shorter in the mutant mice than controls (arrows, Fig. 4E, F).

Figure 4. Ultrastructural abnormalities in the skin of the *Elovl4⁻/⁻* mice. (A, B) Electron micrographs of the wild type (A), and the mutant (B) stratum corneum. The SC in the mutant is more compacted than the control, which has space between each sub-layer. (C, D) Enlarged images of the boxed areas in (A and B). Arrows point to the lamellar membrane between the stratum spinosum and the stratum granulosum. (E, F) Basement membrane in *Elovl4⁻/⁻* mice (F) had fewer hemidesmosomes with shortened or missing tonofilaments (arrows) than control mice (E). Collagenous fibrils in mutant mice were shorter and sparse than controls (arrowheads). Magnification: A, B: X23,457; C, D: X51,605; and E, F: X29,280.
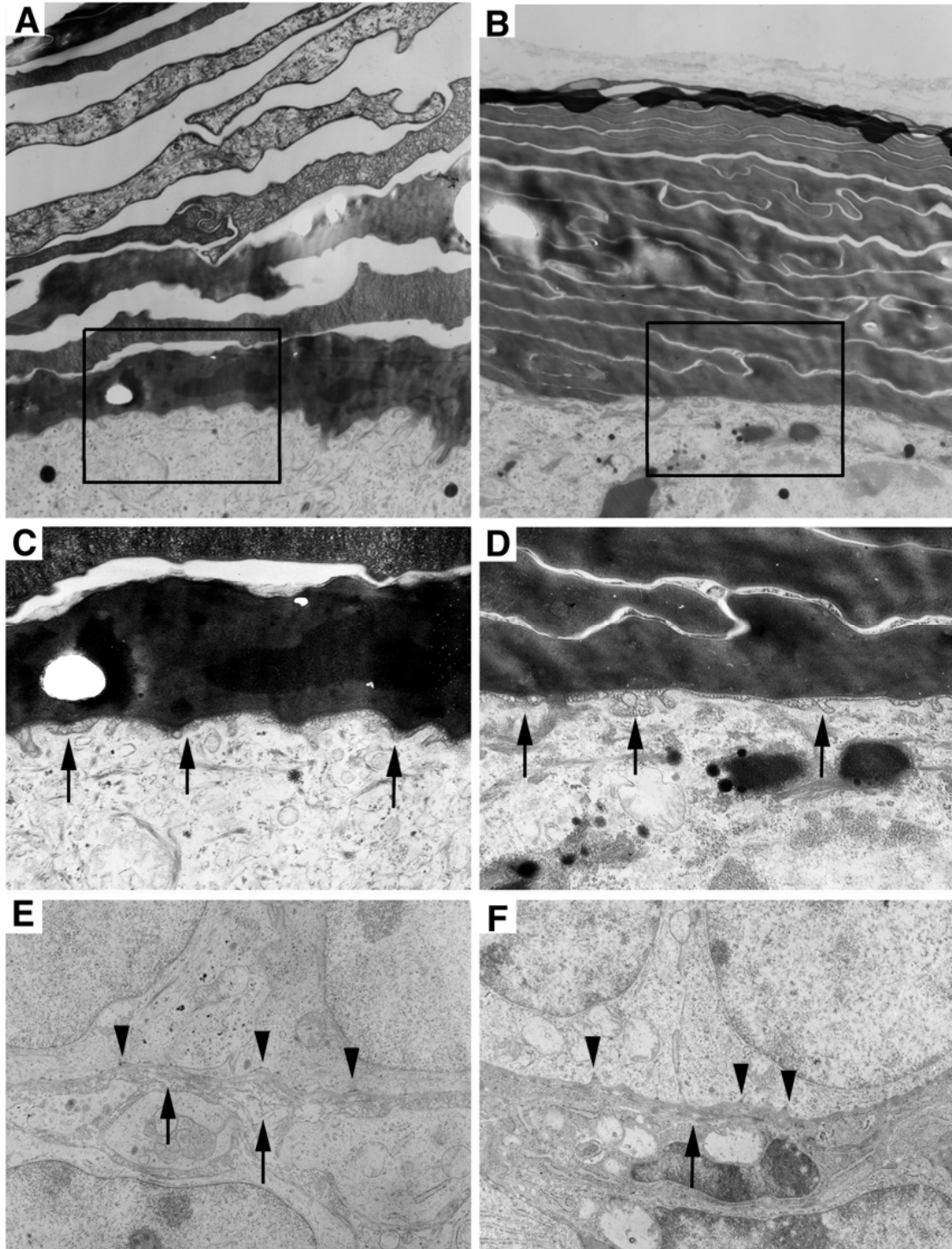
Figure 5. Expression of ceramides with different length fatty acids in the epidermis of the *Elovl4⁻/⁻* mice. Total epidermal ceramides from *Elovl4⁻/⁻* (null), heterozygous (ht) and wild-type (wt) mice with different fatty acid chain lengths (C16-25, C26, C28, C30-36) were quantified by nanoESI-MS/MS. The results are expressed as percentage of total ceramides.
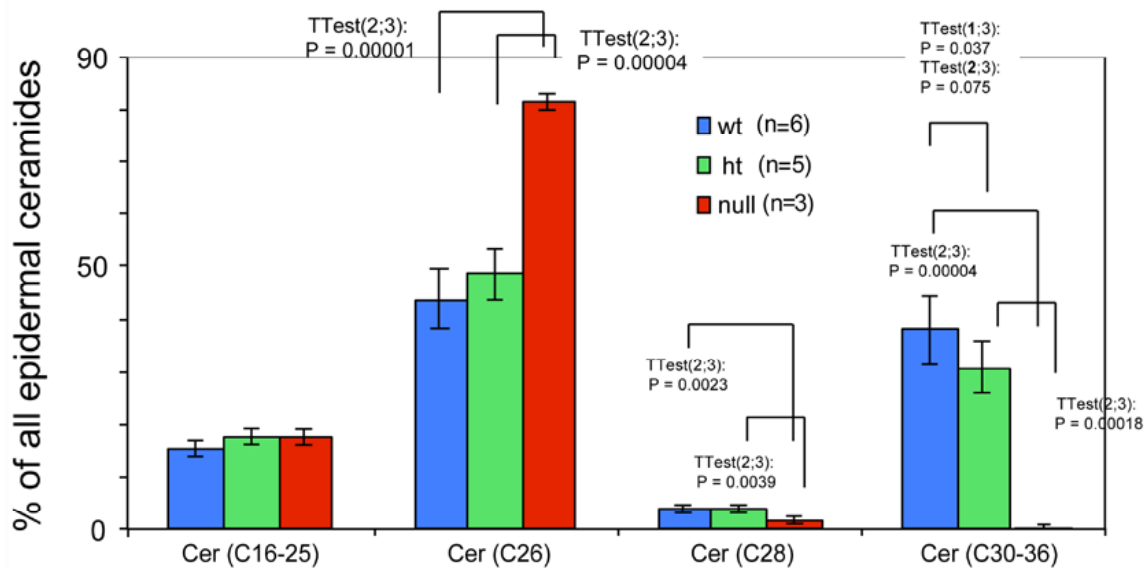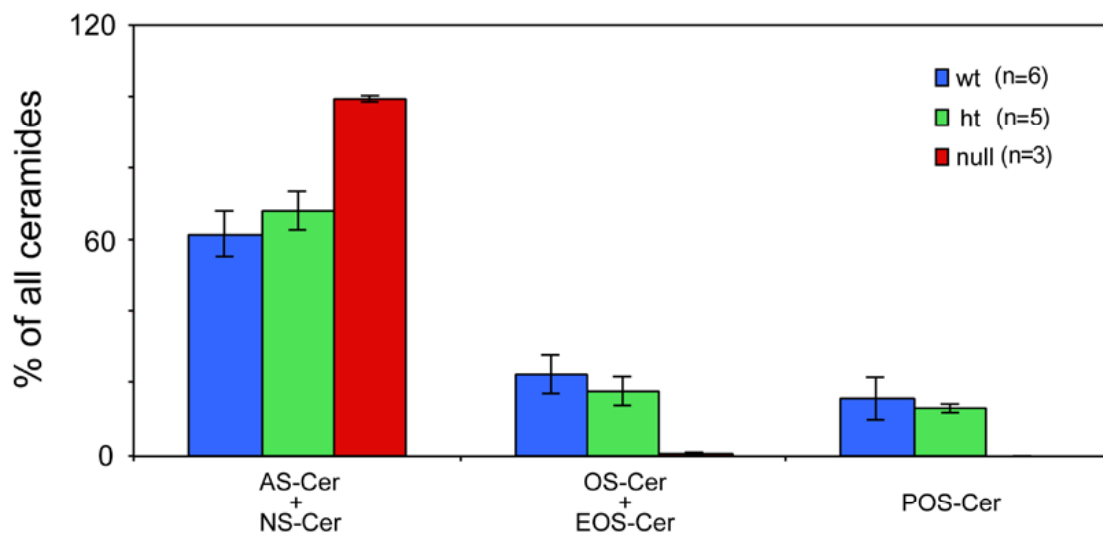

Figure 6. Expression of ceramides with ω- hydroxy fatty acids in in the epidermis of the *Elovl4⁻/⁻* mice. The following ceramide species were quantified from epidermis of *Elovl4⁻/⁻* (null), heterozygous (ht) and wild-type (wt) mice by nanoESI-MS/MS: ceramides containing ω-hydroxy fatty acids (OS), ceramides containing ω-hydroxy fatty acids esterified to linoleic acid (EOS), ceramides containing ω-hydroxy fatty acids bound to protein (POS), ceramides containing non-hydroxy fatty acids (NS) and ceramides containing α-hydroxy fatty acids (AS). The results are expressed as the percentage of total ceramides.

Depletion of ceramides with ω-hydroxy very long fatty acids in the *ELOVL4* deficient mice

Ceramides containing ω-hydroxy very long chain fatty acids are essential components of the epidermal permeability barrier. These can be expressed as free (OS), linoleic acid esterified (EOS) and in protein bound (POS) forms. In the *Elovl4⁻/⁻* epidermis, mass spectrometric analysis revealed that ceramides containing fatty acids longer than C28 (C30-36) were absent, and those with C28 fatty acids were substantially reduced compared with controls (Fig. 5).

These included ω-hydroxyceramides (OS, POS and EOS) that were found in wild-type and heterozygote epidermis with fatty acid lengths equal or longer than C28 (Fig. 6). In contrast, the *Elovl4⁻/⁻* epidermis contained predominantly non-hydroxy (NS)-, α-hydroxy (AS)-ceramides with C26 as longest fatty acid (Fig. 5 and 6). Interestingly, the amount of these ceramides with C26 fatty acids was nearly double the amount in *Elovl4⁻/⁻* mice compared with the wild-type and heterozygous mice (Fig. 5), while the amounts of ceramides with C16-25 fatty acids were similar in the

three genotypes, indicating that the absence of ELOVL4 caused an accumulation of NS- and AS-ceramides with C26 fatty acids.

4. Discussion

EVOVL4 is highly expressed in the human retina and was initially discovered as the causal gene of STGD3 [13]. Consistently, mutant mice carrying the dominant negative form of human *ELOVL4* gene that was either introduced through a knock-in approach ($Elovl4^{+/del}$), or transgenic approach (*IRBP-ELOVL4*) developed early onset of progressive photoreceptor degeneration ([18,19], Li and Deng unpublished data). In contrast, mice heterozygous for a conventional knockout of ELOVL4 developed normally and exhibited no symptoms mimicking human STGD3 [21]. Furthermore, $Elovl4^{-/-}$ mice died unexpected shortly after birth, suggesting that ELOVL4 may play additional functions in other organs/tissues that are critical for early postnatal survival. In addition to the eye, ELOVL4 is also presented at high levels in the skin and brain [12]. Our analysis of $Elovl4^{-/-}$ mice revealing the abnormal differentiation of keratinocytes, and malformation of the SC of the skin indicate that ELOVL4 indeed have critical functions in other organs in addition to the eye.

The SC of the skin serves as a permeability barrier for protecting the internal milieu against the external environment. Previous investigations indicated that mutant mice with malformation of the SC died of dehydration shortly after birth [24-26], establishing that the water barrier function of the SC is critical for postnatal survival. Our data revealed that the SC of $Elovl4^{-/-}$ mice failed to protect against body water evaporation and dye penetration. The mutant SC is thinner and more compact than that of control mice. It also displayed ultrastructural abnormalities and detached from the mutant mice. These observations are consistent with a view that that the $Elovl4^{-/-}$ mice died of dehydration.

Despite the high level of ELOVL4 expression in the brain [12], our examination failed to reveal an obvious histological/morphological difference between mutant and control mice. Of note, we found that the $Elovl4^{-/-}$ mice showed no desire to find the nipple and to suck milk of their mothers. Consequently, all the mutant mice did not drink any milk until their death. Our study ruled out that starvation could be a cause for the lethality, as feeding of mutant mice with milk does not extend their life beyond 6 hours. Meanwhile, the $Elovl4^{-/-}$ mice also had very little body movement. We suspect these phenotypes reflect a neurological behavior abnormality due to the absence of ELOVL4 in the brain. Studies using lineage and molecular markers should be performed in the future to detect alterations in cellular and molecular levels to provide an explanation for these abnormalities.

A key finding to explain the early death of the $Elovl4^{-/-}$ mice was the absence of ceramides with ω-hydroxy very long chain fatty acids in the epidermis of the mutant mice. This finding uncovered an indispensable role for ELOVL4 in the formation of the very long chain fatty acids that serve as constituents of sphingolipids in the epidermal barrier. The lipid barrier that is found on the surface of corneocytes in stratum corneum provides epidermal permeability barrier function, and is required for terrestrial life [3,24-26]. The lipid barrier expresses ceramides as major components, with ceramides containing ω-hydroxyl very long chain fatty acids comprising a significant fraction of epidermal ceramides. Together with a deficiency of ceramides containing fatty acids longer than C28, was the relative accumulation of ceramides containing C26 fatty acids. These results suggest that C26 fatty acids are substrates for ELOVL4 and that ω-hydroxylation probably occurs on fatty acids of chain length C28 or longer. It is plausible that the absence of ≥C28 fatty acids in ELOVL4 null epidermis blocked the synthesis of ceramides with ω-hydroxy fatty acids and, consequently, and their linkage to linoleic acid and protein.

So far six members of ELOVL (ELOVL1-6) have been identified and these enzymes exhibit spatially and temporally specific expression [9]. It was reported that *Elovl3* gene expression in mouse skin was restricted to the sebaceous glands and the epithelial cells of the hair follicles [27]. The disruption of the *Elovl3* gene in mouse resulted in a sparse hair coat, the hyperplasia of the sebaceous glands, and the increased level of eicosenoic acid (20:1) in hair lipids [27]. The result showed that ELOVL3 participates in the formation of neutral lipids bound with fatty acids longer than C20 that are necessary for skin function. These studies revealed that ELOVL3 and ELOVL4 have distinct functions in the skin.

While our work is completed, a study using the skin of $Elovl4^{del/del}$ mice was published online [28]. In that study, Basireddy et al. revealed a similar defect in skin permeability due to the depletion of fatty acids ≥C28 in the mutant SC. However, immunofluorescence using epidermal markers did not detect any obvious differences between the $Elovl4^{del/del}$ and control mice [28]. A plausible explanation is that the $Elovl4^{del/del}$ mice still express the mutant form of ELOVL4 that is 51aa shorter than the full-length protein (314aa). The dominant-negative nature of this mutant form of ELOVL4 might be a cause for the observed differences between the $Elovl4^{del/del}$ and $Elovl4^{-/-}$ mice. This issue deserves further investigations in the future.

Similar phenotypes were found in mice carrying either a null mutation of ELOVL4 ($Elovl4^{-/-}$) or a truncation of ELOVL4 at 270aa ($Elovl4^{270X/270X}$) [29], which appears in the same issue of the International Journal of Biological Sciences.

Acknowledgements

Conflict of interest

The authors have declared that no conflict of

interest exists.

References

1. Mack JA, Anand S, andMaytin EV. Proliferation and cornification during development of the mammalian epidermis. Birth Defects Res C Embryo Today 2005 75:314-29.
2. Fuchs E, andRaghavan S. Getting under the skin of epidermal morphogenesis. Nat Rev Genet 2002 3:199-209.
3. Bouwstra JA, Honeywell-Nguyen PL, Gooris GS, et al. Structure of the skin barrier and its modulation by vesicular formulations. Prog Lipid Res 2003 42:1-36.
4. Rissmann R, Groenink HW, Weerheim AM, et al. New insights into ultrastructure, lipid composition and organization of vernix caseosa. J Invest Dermatol 2006 126:1823-33.
5. Kalinin AE, Kajava AV, and Steinert PM. Epithelial barrier function: assembly and structural features of the cornified cell envelope. Bioessays 2002 24:789-800.
6. Madison KC. Barrier function of the skin: "la raison d'etre" of the epidermis. J Invest Dermatol 2003 121:231-41.
7. Holleran WM, Takagi Y, and Uchida Y. Epidermal sphingolipids: metabolism, function, and roles in skin disorders. FEBS Lett 2006 580:5456-66.
8. Doering T, Brade H, and Sandhoff K. Sphingolipid metabolism during epidermal barrier development in mice. J Lipid Res 2002 43:1727-33.
9. Jakobsson A, Westerberg R, and Jacobsson A. Fatty acid elongases in mammals: their regulation and roles in metabolism. Prog Lipid Res 2006 45:237-49.
10. Lagali PS, Liu J, Ambasudhan R, et al. Evolutionarily conserved ELOVL4 gene expression in the vertebrate retina. Invest Ophthalmol Vis Sci 2003 44:2841-50.
11. Umeda S, Ayyagari R, Suzuki MT, et al. Molecular cloning of ELOVL4 gene from cynomolgus monkey (Macaca fascicularis). Exp Anim 2003 52:129-35.
12. Mandal MN, Ambasudhan R, Wong PW, et al. Characterization of mouse orthologue of ELOVL4: genomic organization and spatial and temporal expression. Genomics 2004 83:626-35.
13. Zhang K, Kniazeva M, Han M, et al. A 5-bp deletion in ELOVL4 is associated with two related forms of autosomal dominant macular dystrophy. Nat Genet 2001 27:89-93.
14. Edwards AO, Donoso LA, and Ritter R 3rd. A novel gene for autosomal dominant Stargardt-like macular dystrophy with homology to the SUR4 protein family. Invest Ophthalmol Vis Sci 2001 42:2652-63.
15. Bernstein PS, Tammur J, Singh N, et al. Diverse macular dystrophy phenotype caused by a novel complex mutation in the ELOVL4 gene. Invest Ophthalmol Vis Sci 2001 42:3331-6.
16. Griesinger IB, Sieving PA, and Ayyagari R. Autosomal dominant macular atrophy at 6q14 excludes CORD7 and MCDR1/PBCRA loci. Invest Ophthalmol Vis Sci 2000 41:248-55.
17. Kniazeva MF, Chiang MF, Cutting GR, et al. Clinical and genetic studies of an autosomal dominant cone-rod dystrophy with features of Stargardt disease. Ophthalmic Genet 1999 20:71-81.
18. Karan G, Lillo C, Yang Z, et al. Lipofuscin accumulation, abnormal electrophysiology, and photoreceptor degeneration in mutant ELOVL4 transgenic mice: a model for macular degeneration. Proc Natl Acad Sci U S A 2005 102:4164-9.
19. Vasireddy V, Jablonski MM, Mandal MN, et al. Elovl4 5-bp-deletion knock-in mice develop progressive photoreceptor degeneration. Invest Ophthalmol Vis Sci 2006 47:4558-68.
20. Yang X, Li C, Herrera PL, et al. Generation of Smad4/Dpc4 conditional knockout mice. Genesis 2002 32:80-1.
21. Li W, Chen Y, Cameron DJ, et al. Elovl4 haploinsufficiency does not induce early onset retinal degeneration in mice. Vision Research 2007 [Epub ahead of print].
22. Jennemann R, Sandhoff R, Langbein L, et al. Integrity and barrier function of the epidermis critically depend on glucosylceramide synthesis. J Biol Chem 2007; 282:3083-3094.
23. Sandhoff R, Hepbildikler ST, Jennemann R, et al. Kidney sulfatides in mouse models of inherited glycosphingolipid disorders: determination by nano-electrospray ionization tandem mass spectrometry. J Biol Chem 2002 277:20386-98.
24. Matsuki M, Yamashita F, Ishida-Yamamoto A, et al. Defective stratum corneum and early neonatal death in mice lacking the gene for transglutaminase 1 (keratinocyte transglutaminase). Proc Natl Acad Sci U S A 1998 95:1044-9.
25. Yang T, Liang D, Koch PJ, et al. Epidermal detachment, desmosomal dissociation, and destabilization of corneodesmosin in Spink5-/- mice. Genes Dev 2004 18:2354-8.
26. Hewett DR, Simons AL, Mangan NE, et al. Lethal, neonatal ichthyosis with increased proteolytic processing of filaggrin in a mouse model of Netherton syndrome. Hum Mol Genet 2005 14:335-46.
27. Westerberg R, Tvrdik P, Unden AB, et al. Role for ELOVL3 and fatty acid chain length in development of hair and skin function. J Biol Chem 2004 279:5621-9.
28. Vasireddy V, Uchida Y, Salem N, et al. Loss of functional ELOVL4 depletes very long-chain fatty acids (>=C28) and the unique {omega}-O-acylceramides in skin leading to neonatal death. Hum Mol Genet 2007 [Epub ahead of print].
29. Cameron DJ, Tong Z, Yang Z, et al. Essential role of Elovl4 in very long chain fatty acid synthesis, skin permeability barrier function, and neonatal survival. Int J Biol Sci. 2007, 3:111-119.